Enriquez et al. Supplementary Data

Supplementary data include supplementary material and methods, 20 supplementary figures and 3 supplementary tables.

An additional file showing uncropped western blot gels (relative to supplementary figures 4B, 5C, 6H, 7G, S1E, S3B, S7A and D) is included.

SUPPLEMENTRAY MATERIAL AND METHODS

Cell culture media

All murine cells were cultured in DMEM (Gibco) supplemented with 10% of fetal bovine serum (Gibco), 2 mmol/L L-glutamine, 150 U/mL streptomycin, and 200 U/mL penicillin (Cambrex), 10 mmol/L Hepes and 10 mmol/L sodium pyruvate (Gibco). Human cell lines were maintained in RPMI (Gibco) supplemented with 10% of fetal bovine serum (Gibco), 2 mmol/L L-glutamine, 150 U/mL streptomycin, and 200 U/mL penicillin (Cambrex), 10 mmol/L Hepes and 10 mmol/L sodium pyruvate (Gibco) and 2.5g/L glucose (Sigma).

Sparc reporter Assay

The sequence of Sparc 3'UTR, extrapolated on the Genome Browser website (RRID:SCR_004267) is here reported:

(gttcacgcctcctgctgcagtcctgaactctctccctctgatgtgtccccctcccattacccccttgtttaaaatgtttggatg gttggctgttccgcctggggataaggtgctaacatagatttaactgaatacattaacggtgctaaaaaaaaaaaaaaaa),

Instrument setting for confocal microscopy

For pSTAT3 immunofluorescence imaging was performed using a confocal laser-scanning microscope Leica TCS SP8 X (Leica Microsystems), equipped with a pulsed super continuum White Light Laser (470-670nm; 1nm tuning step size). Laser lines were 495 nm for FITC and alexa fluor 488, 556 nm for alexa fluor 546 and 633 nm for APC; detection range were 501nm to 556 nm, 569 to 630 nm and 638 to 744 nm, respectively. Images were acquired in the scan format 1024x1024 pixel using a HC PL APO 63X/1.40 CS2 oil immersion objective and a pinhole set to 1 Airy unit. Data were analyzed using the software Leica LASX rel.1.1 (Leica Microsystems) and the Image J software (RRID:SCR_003070).

Cytospin

Cells were detached and suspended at 10^5/100 µl. Glass slides were mounted with paper pad and cuvettes with a metal holder, loaded with 100 µl of cell suspension and spinned 2 minutes at 2000 rpm with a cytocentrifuge. After detaching of cuvettes and filters, slides were dried overnight and then fixed for 20 minutes with PBS containing 2% PFA. For immunofluorescence, after permeabilization for 10 minutes with PBS containing 0.5% Saponin (Sigma) and blocking with PBS containing 5% BSA we followed the protocol described for FFPE tumor sections.

List of Taqman probes used for Real-time PCR

All listed Taqman probes are from Applied Biosystems.

Probes for mouse samples: *Ar* (Mm00442688_m1), *Syp* (Mm00436850_m1), *Krt8* (Mm00835759_m1), *Sparc* (Mm00486332_m1), *Il6* (Mm00446190_m1), *Hspa5* (GRP78; Mm00517691_m1), *Ctnbb1* (β-catenin; Mm00483039_m1) and *Gapdh*

(Mm99999915_g1). Probes for human samples: *Ctnbb1* (β-catenin; Hs00355045_m1), *Cga* (Chromogranin A; Hs00900375_m1), *Eno2* (Enolase-2; Hs00157360_m1), and *Gapdh* (Hs02786624_g1). Probes for miRNA detection: *miR-29b1* (mmu-miR-29b-3p; cat. 000413), *U6* (U6 snRNA; cat. 001973) or cel-miR-39 (cel-miR-39-3p; cat. 000200).

Flow cytometry

Table S1 provides the list of all antibodies used in flow cytometry experiments with T23 and T1525 cells or with cell-suspensions obtained from collagenase-digested prostates. Staining was performed incubating cells for 15' at 4°C. 7AAD (eBioscience) was added to exclude dead cells. For evaluation of intracellular phosphorylated STAT3 (pSTAT3), T1525 and T23 cells were stimulated for 30 minutes with 50 ng/ml of recombinant murine IL6 (cat. no. 216-16, Peprotec), in presence or not of a monoclonal antibody to IL6-R (50 ng/ml; D7715A7 clone, Table S1) or of isotype control (50 ng/ml, Table S1). Cells were then fixed with IC-Fix Buffer (eBiosciences), permeabilized with ice-cold methanol and stained according to the BD-Phosflow kit protocol (BD-Biosciences).

Exosomes to be analyzed by flow cytometry were conjugated with latex beads (Aldehyde/Sulfate latex, 4% w/v 4 μm; ThermoFisher). Briefly, exosomes were incubated 15 min at room temperature with 10 μl of beads, then a volume of 900 μl of PBS was added prior to incubation overnight on a tube rotator wheel at 4°C. Samples were then incubated with 100 mM glycine for 30 min at room temperature, and, after washing, they were incubated with PBS-5%BSA for 30 min at room temperature. After washing, samples were then stained with APC anti CD63 antibody (Table S1).

Samples were acquired with BD LSRII Fortessa™ and analyzed with the Flow Jo software (RRID:SCR_008520).

ELISA

IL-6 in cultures supernatants was detected using the Invitrogen mouse or human IL-6 ELISA Kit (cat. no. BMS603-2TWO and cat.no 88-7066-22, respectively), according to the manufacturer protocol.

Western Blot

Cells were lysed in RIPA buffer (Cell Signaling Technologies). Lysates (20 or 50 ng/ sample) were run on NuPAGE Bis- Tris gels (4%-12% polyacrylamide; Invitrogen by ThermoFisher) and transferred on a nitrocellulose membrane (GE Healthcare). After blocking 1h at room temperature with 5% BSA diluted in PBS 0.5% Tween, the membrane was incubated overnight at 4°C with primary antibody. HRP conjugated secondary antibody was then incubated 1h at room temperature. All antibodies used are listed in Table S1. Staining was revealed with ECL solution (GE Healthcare) and developed of an X-ray film or acquired with the ChemiDoc MP Imaging System (Bio-Rad). Quantification of staining intensity was performed with the ImageJ software (RRID:SCR_003070), and reported as fold change relative to internal control (β-actin or vinculin).

RNA-Sequencing

Total RNA was isolated from cell lines by means of miRNeasy Tissue/Cells Advanced Mini Kit (QUIAGEN) according to the manufacturer's protocol. RNA quality and quantity were checked using Agilent 2100 Bioanalyzer (Agilent

Technologies, Santa Clara, California, U.S.) and Nanodrop spectrophotometer (ThermoFisher,). 500 ng of totRNA were used to prepare RNA libraries by means of the TruSeq Stranded mRNA Library Prep Kit (Illumina, San Diego, California, U.S.) following the manufacturer's protocol. Briefly, the mRNA fraction was purified from total RNA by polyA capture, fragmented and subjected to first-strand cDNA synthesis with random primers in the presence of Actinomycin D. The second-strand synthesis was performed incorporating dUTP instead of dTTP. Then a single 'A' nucleotide was added to the 3' ends of the blunt fragments to prevent them to ligating to each other. Index adapters were ligated and cDNA was subjected to PCR amplification. Libraries were validated using Agilent bioanalyzer (DNA 1000 kit) and the concentration was evaluated by means of Qubit™ dsDNA HS Assay Kit (ThermoFisher). Libraries were normalized, multiplexed and sequenced on the Illumina NextSeq 550 system. Bcl files were demultiplexed using the bcl2fastq tool v 2.20.0.422. Raw sequence reads (fastq) underwent quality control by means of FastQC 0.11.9. Trimming was performed with Cutadapt 2.9 (RRID:SCR_011841). Alignment was performed using STAR 2.6.1d against the mouse GRCm38 reference genome and reads were counted by means of FeatureCounts 2.0 (RRID:SCR_012919), asking for a gene-level report. Finally, the DeSeq2 package (RRID:SCR_015687), available within Bioconductor, was used to normalize count data, estimate biological variance and determine differential expression. RNAseq data have been deposited to GEO (RRID:SCR_004584), the accession number is GSE156033. Log2Fold-changes and Ajusted p-values were generated for each class comparison (Table S2).

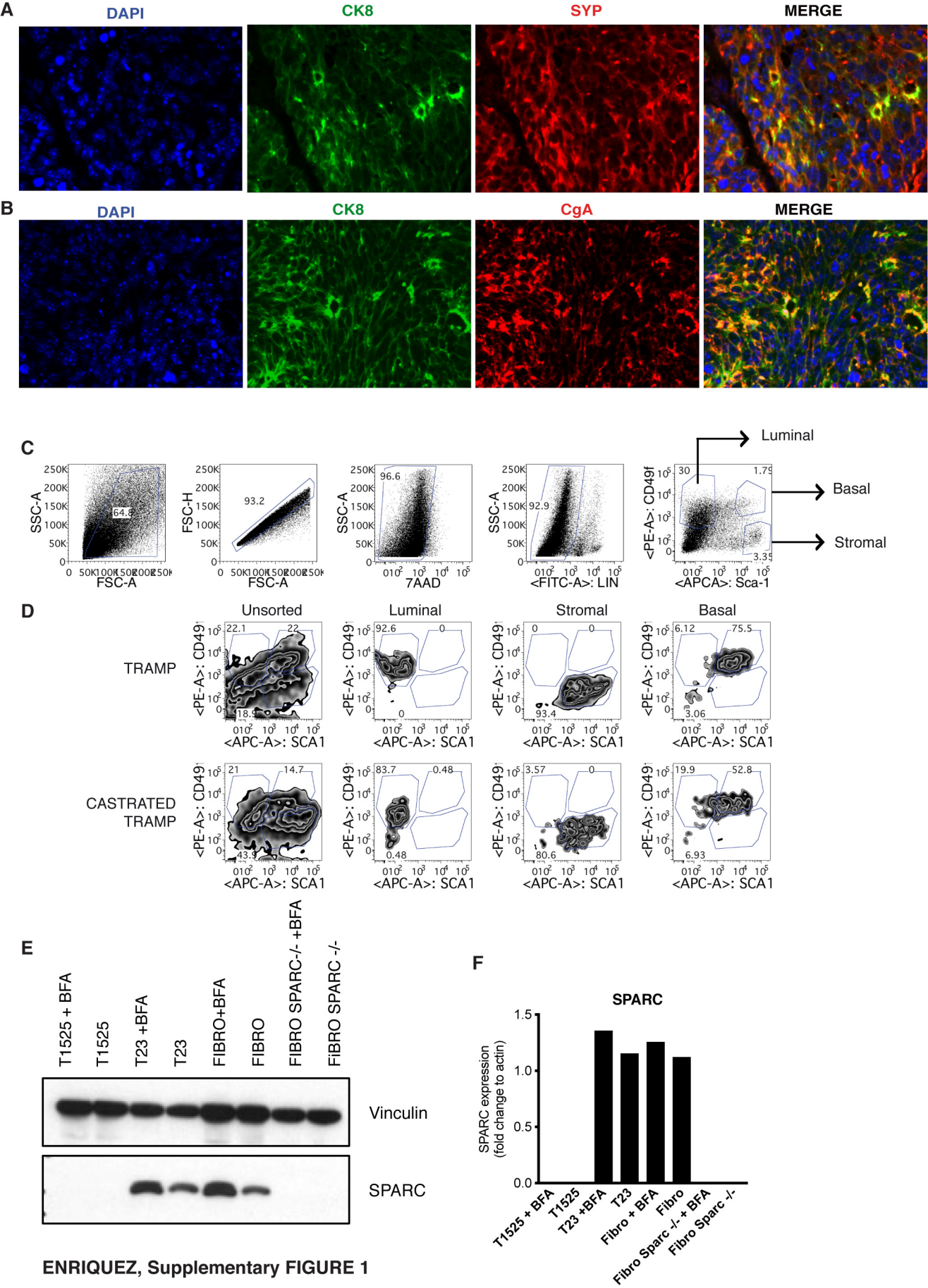

ENRIQUEZ, Supplementary FIGURE 1

SUPPLEMENTARY FIGURES

Supplementary Figure 1. Luminal and basal cell sorting from TRAMP prostates and SPARC expression by in vitro cell lines A. Enlarged digital magnification for immunofluorescence reported in figure 1C. Green: CK8, Red: SYP, Blue: DAPI. **B.** Enlarged digital magnification for immunofluorescence reported in figure 1E. Green: CK8, Red: CgA, Blue: DAPI **C.** Representative dot plots indicating the gating strategy adopted for sorting of luminal ($Lin^-CD49f^+Sca\text{-}1^-$) and stromal ($Lin^-CD49f^-Sca\text{-}1^+$) cells from prostates of TRAMP, $Sparc^{-/-}$TRAMP or castrated TRAMP mice, as indicated in the text. Lin: Ter119, CD31, CD45. Dead cells were excluded with 7AAD staining. This gated strategy allows also the identification of basal cells ($Lin^-CD49f^+Sca\text{-}1^+$), which were not further analyzed. **D.** Dot plots showing purity of cells recovered after sorting. **E.** Western blot for SPARC in cell lysates from T1525 and T23 tumor cell lines and in fibroblast obtained from wild type (Fibro) or Sparc-/- mice (Fibro SPARC-/-). Where indicated cell were treated with brefeldin A (BFA) to prevent proteins secretion. Vinculin was used as internal control. The western blot was validated twice. **F.** Quantification of E.

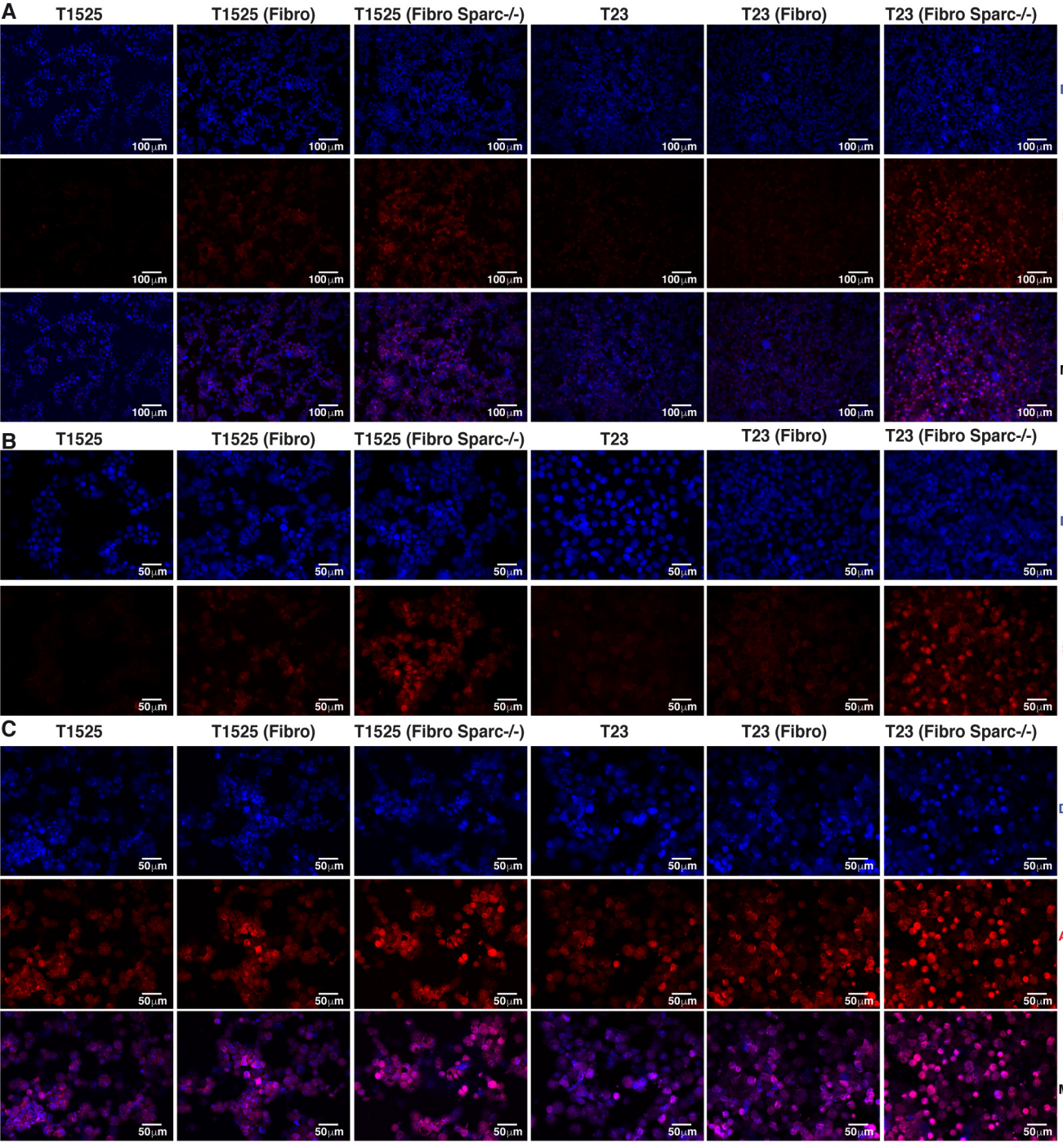

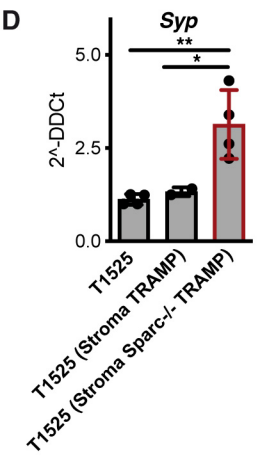

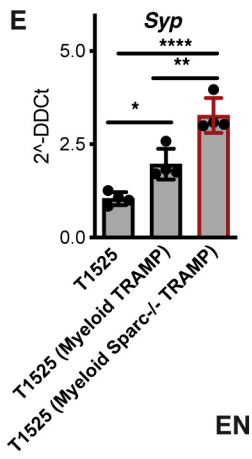

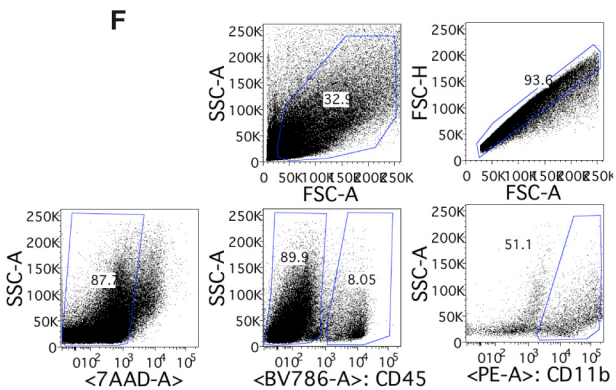

ENRIQUEZ, Supplementary FIGURE 2

Supplementary Figure 2. Stroma cells from Sparc$^{-/-}$TRAMP mice induce NED of adenocarcinoma. A and B. Enlarged fields (A) and separate channels (B) for immunofluorescence reported in figure 2C and 2D. Red: SYP, Blue: DAPI. **C.** Immunofluorescence for AR (red) in tumor cells treated as in figure 2A and B. Blue: DAPI. **D and E.** T1525 prostate adenocarcinoma cell lines were co-cultured with stromal cells (D; sorted as in Fig. S1) or CD11b^{+} myeloid cells (E), as indicated in brackets, isolated from prostates of TRAMP and Sparc$^{-/-}$TRAMP mice. Cells were divided by a 0.4 μm pore transwell, and analyzed after 7 days of culture. Graphs show real time PCR for *Syp* on tumor cells. Data are a pool of two independent experiments. Histograms depict mean ± s.d. of biological replicates. One-Way Anova followed by Tukey's test: * $P < 0.05$, ** $P < 0.01$, **** $P < 0.0001$. **F.** Representative dot plots indicating the gating strategy adopted for isolation of CD11b^{+} cells from prostates of TRAMP and Sparc$^{-/-}$TRAMP mice, as indicated in the text. Dead cells were excluded with 7AAD staining.

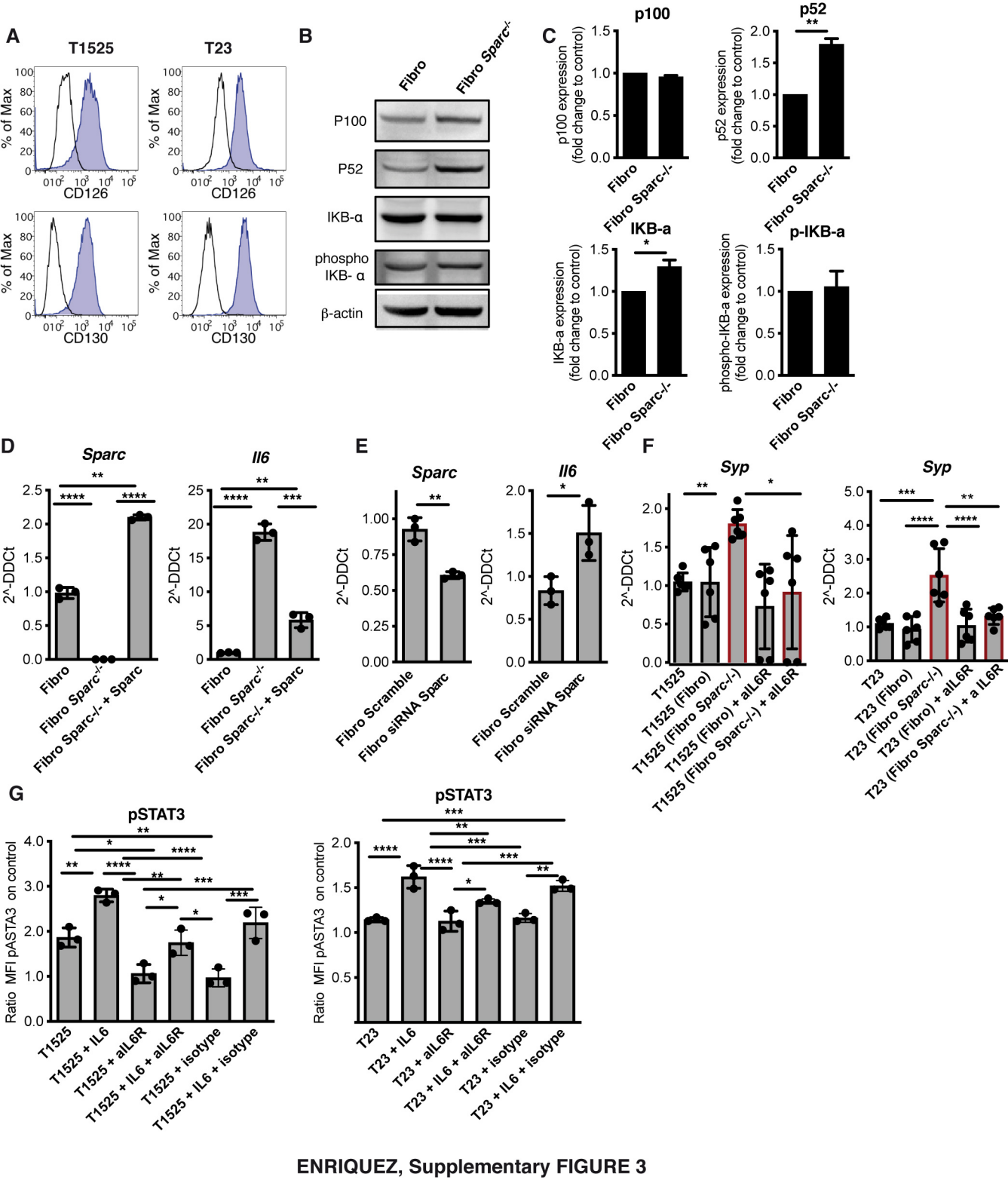

ENRIQUEZ, Supplementary FIGURE 3

Supplementary Figure 3. NED depends on IL-6 release by SPARC-deficient stroma. A. Flow cytometry evaluation of CD126 (IL6R) and CD130 on T1525 and T23 cells. Grey filled histogram: specific staining; black histogram: negative control. **B.** Western blot for p100, p52, IKB-α and phospho IKB-α in cell lysates from wild type (Fibro) or Sparc-/- fibroblasts. β-actin was used as internal control. The western blot was repeated three times. **C.** Quantification of B. Two-tailed Student's t test: * $P < 0.05$, ** $P < 0.01$. **D.** Real time PCR for *Sparc* and *Il6* in fibroblast wild type, $Sparc^{-/-}$ or $Sparc^{-/-}$ in which *Sparc* was re-introduced. **E.** Real time PCR for *Sparc* and *Il6* in wild type fibroblast (Fibro) transiently transfected with Scramble or with siRNA specific for SPARC. **F.** T1525 or T23 cells were cultured with wild type or $Sparc^{-/-}$ fibroblasts, as indicated in brackets, in presence or not of anti-IL6 receptor antibody (αIL6R) as described in Fig. 2I-J. Graphs show real time PCR for *Syp* on tumor cells. Data are a pool of three independent experiments. **G.** Flow cytometry evaluation of phosphorylated STAT3 (pSTAT3) in T1525 or T23 cells stimulated with IL6 in presence or not of αIL6R or isotype control. **E**. Two-tailed Student's t test: * $P < 0.05$, ** $P < 0.01$ **D/F/G.** One-Way Anova followed by Tukey's t, est: * $P < 0.05$, ** $P < 0.01$,*** $P < 0.001$, **** $P < 0.0001$. All histograms depict mean ± s.d. of biological replicates, indicated by dots.

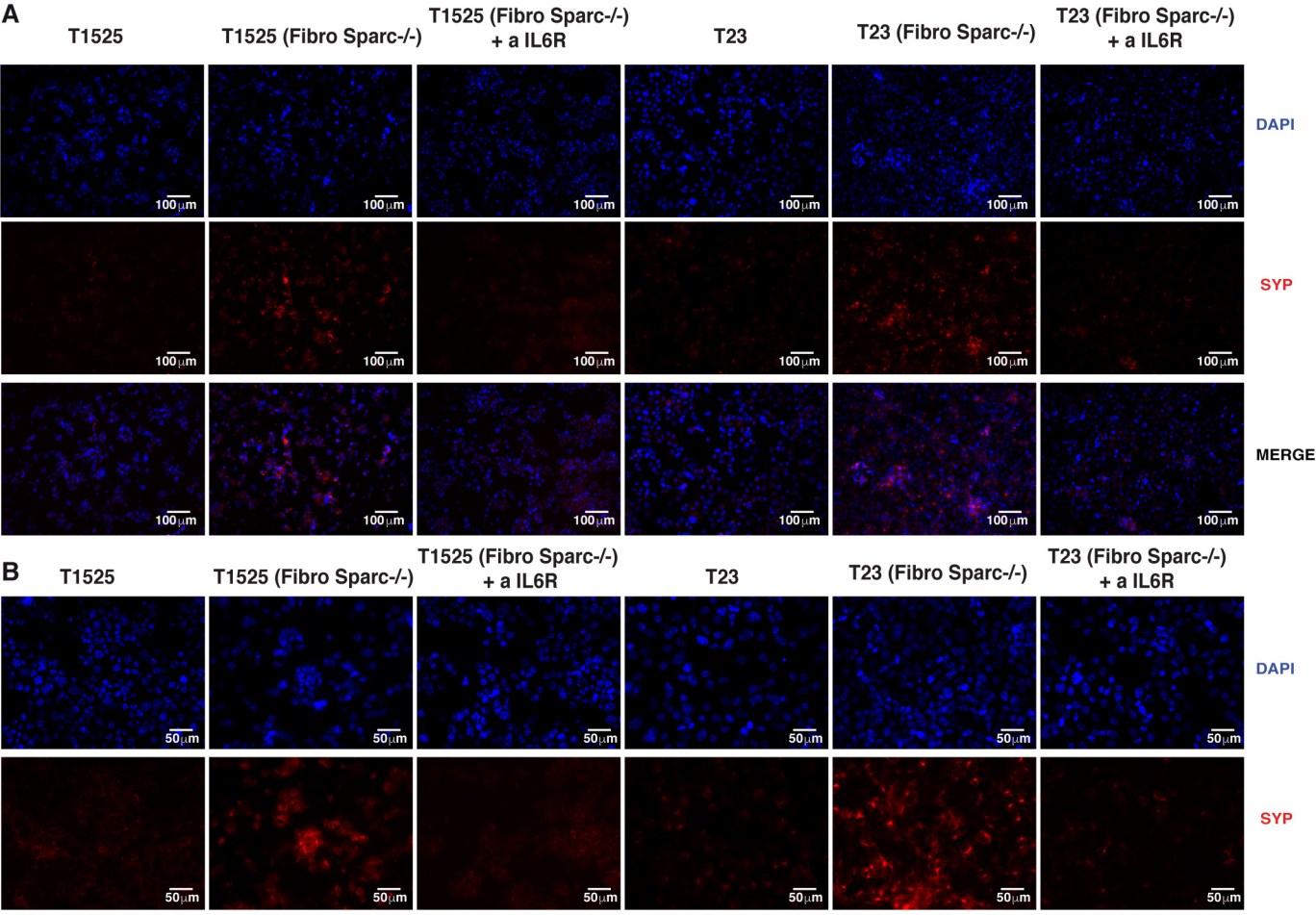

ENRIQUEZ, Supplementary FIGURE 4

Supplementary Figure 4. Blocking IL-6 receptor restrains NED in tumor cells *in vitro*. A and B. Enlarged fields (A) and separate channels (B) for immunofluorescence reported in figure 2I and 2J. Red: SYP, Blue: DAPI.

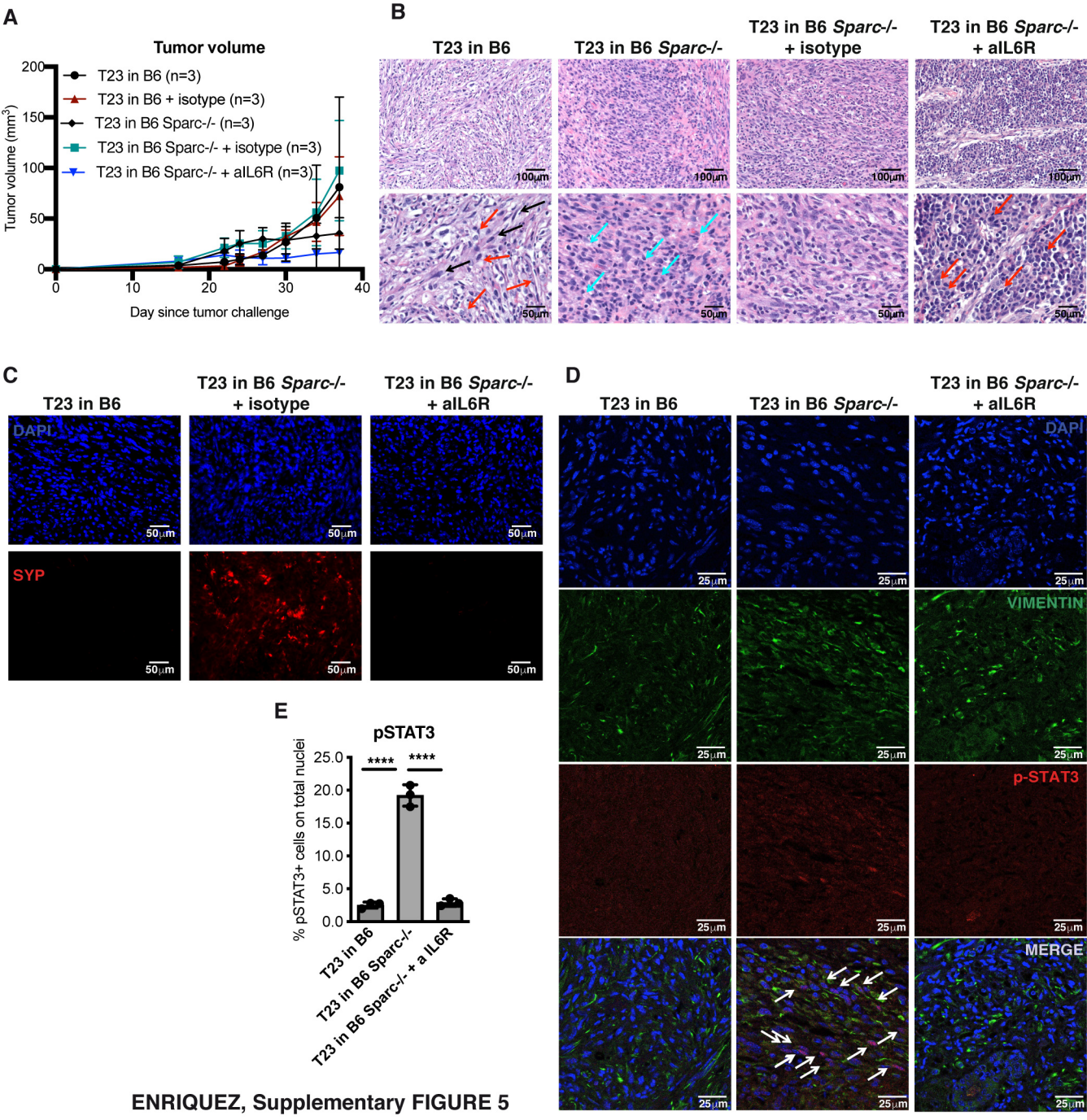

ENRIQUEZ, Supplementary FIGURE 5

Supplementary Figure 5. Blocking IL-6 receptor restrains NED in tumor cells *in vivo*. A. Growth curve of T23-derived tumors grown in wild type (B6) or *Sparc*$^{-/-}$ mice, treated or not with αIL6R or isotype control as indicated in figure 2M. Experiment was repeated two times, each with 3 mice/group, with comparable results. One of the two experiments is shown. **B.** Representative H&E staining of tumors described in A. Black, red or cyan arrows highlight sarcomatoid epitelioid or small-size cells, respectively. **C.** Separate channels for immunofluorescence reported in figure 2M. **D.** Representative immunofluorescence for pSTAT3 (Red) and vimentin (Green) in tumors described in A. Cells positive for pSTAT3 are highlighted with arrows in the merged picture. **E.** Quantification of pSTAT3 staining in D (n=3/group). Histograms depict mean ± s.d. of biological replicates, indicated by dots. One-Way Anova followed by Tukey's test: **** $P < 0.0001$.

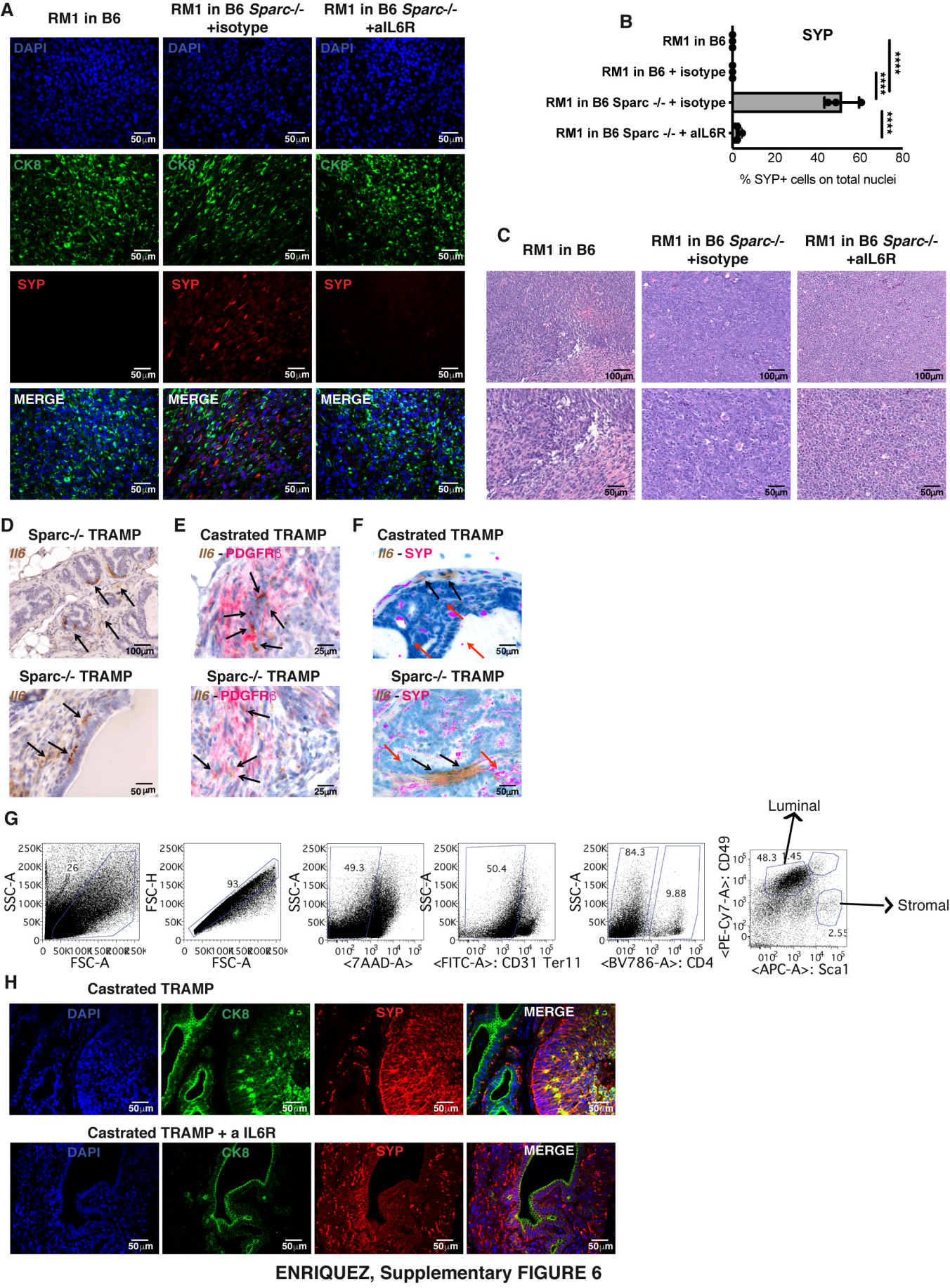

ENRIQUEZ, Supplementary FIGURE 6

Supplementary Figure 6. NED occurs in RM1 tumors grown in *Sparc-/-* hosts. A. Representative immunofluorescence (green: CK8, red: SYP, blue: DAPI) of RM1-derived tumors grown in wild type (B6) or *Sparc-/-* mice, treated or not with αIL6R or isotype control. Experiment was repeated two times, each with 3 mice/group, with comparable results. One of the two experiments is shown **B.** Quantification of SYP immunofluorescence in panel A. Histograms depict mean ± s.d. of biological replicates (n=3/group). One-Way Anova followed by Tukey's test: **** $P < 0.0001$. **C.** Representative H&E staining of tumors described in A. **D.** Representative pictures showing *Il6* RNA evaluation by RNAscope on prostate tissues of *Sparc*$^{-/-}$ TRAMP mice. Black arrows highlight positive cells. **E** Representative pictures showing double stain for *Il6* RNA by RNAscope (signal in brown) and PDGFRβ immunohistochemical staining (signal in fuchsia) in prostates from castrated TRAMP or *Sparc*$^{-/-}$ TRAMP mice. Black arrows indicate double positive cells. **F.** Representative microphotographs showing double stain for *Il6* RNA by RNAscope (signal in brown, highlighted by black arrows) and SYP immunohistochemical staining (signal in fuchsia, highlighted by red arrows) in prostates from castrated TRAMP or *Sparc*$^{-/-}$ TRAMP mice. **G.** Gating strategy for flow cytometry evaluation of CD126 and CD130 (histograms reported in Fig. 3c) on luminal (CD31$^-$CD119$^-$ CD45$^-$CD49f$^+$Sca-1$^-$) and stromal (CD31$^-$CD119$^-$CD45$^-$CD49f$^-$Sca-1$^+$) cells from prostates of TRAMP and castrated TRAMP mice. Dead cells were excluded with 7AAD staining. Experiment was repeated twice. **H.** Immunofluorescence staining for CK8 (green), SYP (red) and DAPI (blue) showing NED on a prostate of a castrated TRAMP mouse and of a castrated TRAMP mouse treated with aIL6R.

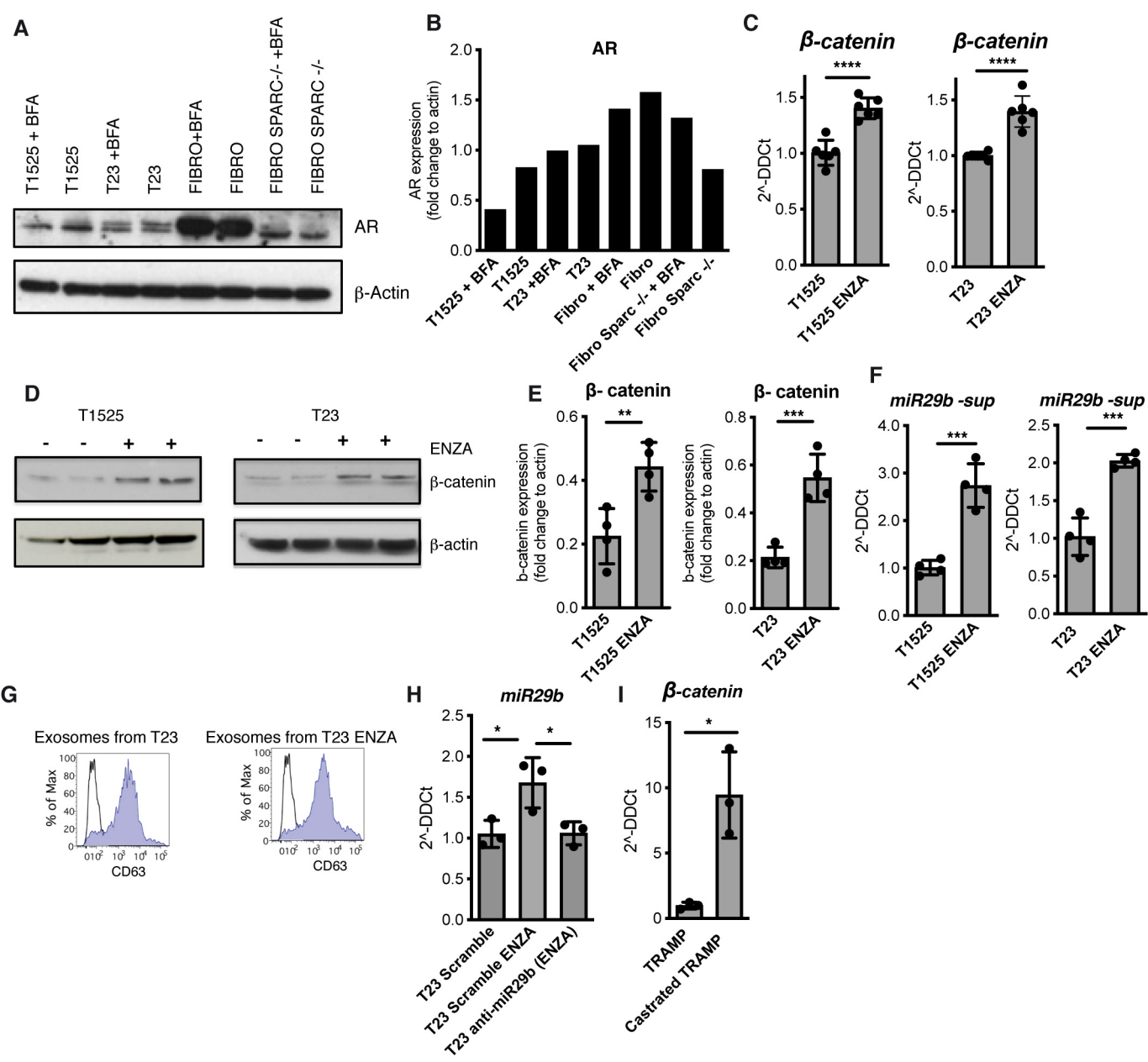

ENRIQUEZ, Supplementary FIGURE 7

Supplementary Figure 7. AR, β-catenin and *miR29b1* expression on fibroblasts and tumor cells. A. Western blot for AR in cell lysates from T1525 and T23 tumor cell lines and in fibroblast obtained from wild type (Fibro) or Sparc-$^{/-}$ mice (Fibro SPARC$^{-/-}$). Where indicated cell were treated with brefeldin A (BFA) to prevent proteins secretion. β-actin was used as internal control. The western blot was validated twice. **B.** Quantification of A. **C-E** Real time PCR (C) and western blot (D) for β-catenin (*Ctnbb1* gene) on T1525 or T23 cells treated with enzalutamide (ENZA) for 24h. Data are a pool of three (C) or two (E) independent experiments. **E.** Quantification of D**. F.** Real time PCR for *miR29b1* on supernatants of T1525 or T23 cells treated with enzalutamide (ENZA) for 24h. Data are a pool of two independent experiments. **G.** Flow cytometry evaluation of CD63 on exosomes isolated from T23 cells, treated or not with enzalutamide (ENZA). **H.** Real time PCR for *miR29b1* in T23 cells transiently transfected with Scramble or with anti-miR specific for *miR-29b* and treated or not with enzalutamide (ENZA). **I.** Real time PCR for β-catenin (*Ctnbb1*) on luminal cells sorted from the prostates of untreated and castrated TRAMP mice (n= 3 biological replicates/group).

All histograms depict mean ± s.d. of biological replicates, indicated by dots. Two-tailed Student's t test: * $P < 0.05$, ** $P < 0.01$,*** $P < 0.001$, **** $P < 0.0001$.

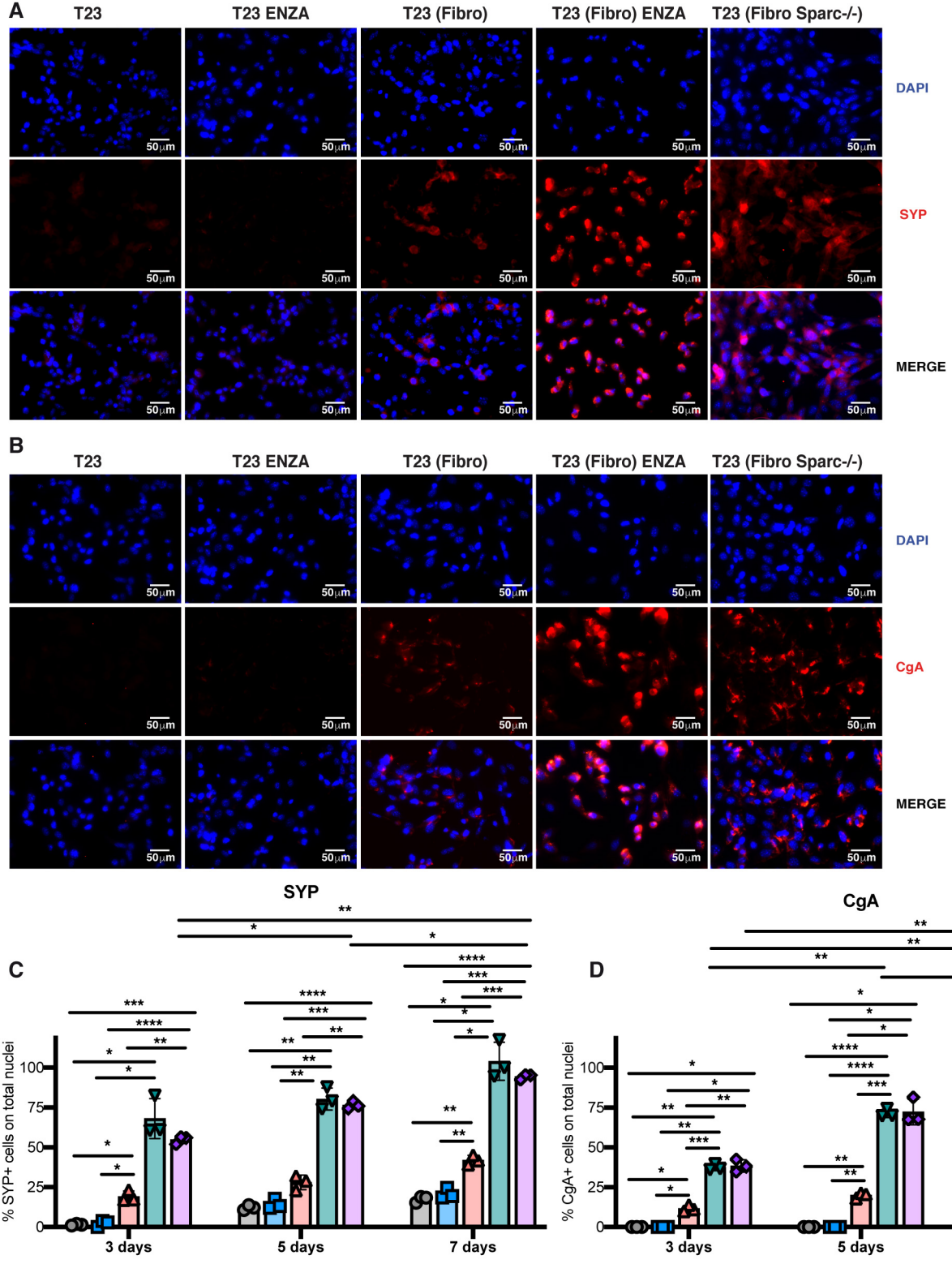

ENRIQUEZ, Supplementary FIGURE 8

Supplementary Figure 8. Co-culture with fibroblasts and enzalutamide causes NED of adenocarcinoma cells. A-D. T23 prostate adenocarcinoma cell lines were co-cultured in transwell system with fibroblasts (Fibro, indicated in brackets) also adding enzalutamide (ENZA), or with Sparc-/- fibroblasts as control. Cells were collected after 3, 5 or 7 days and analyzed by immunofluorescence for SYP (A) or CgA (B). Histograms in **C** and **D** represent digital quantification of SYP and CgA staining, respectively, and depict mean ± s.d. of biological replicates, indicated by dots. Two-Way Anova: * $P < 0.05$, ** $P < 0.01$,*** $P < 0.001$, **** $P < 0.0001$.

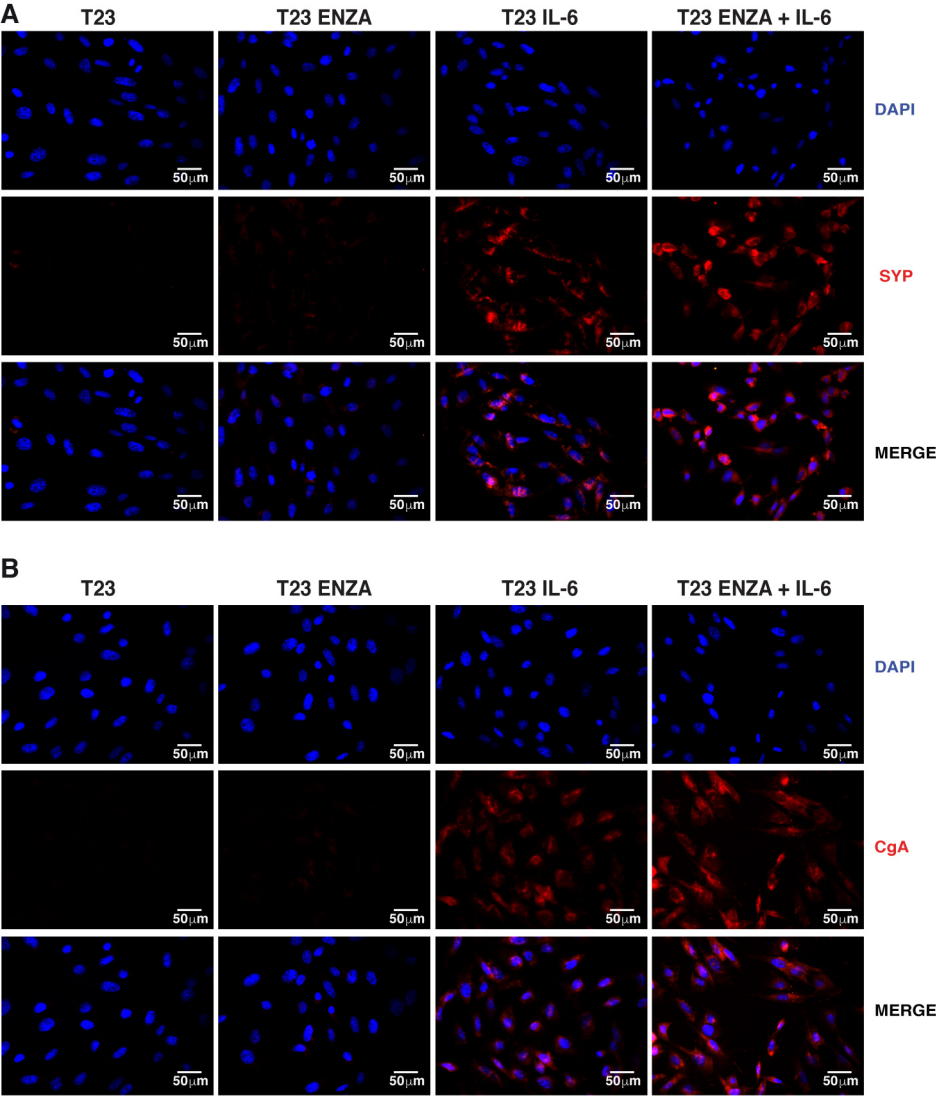

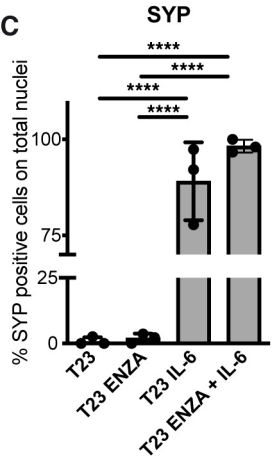

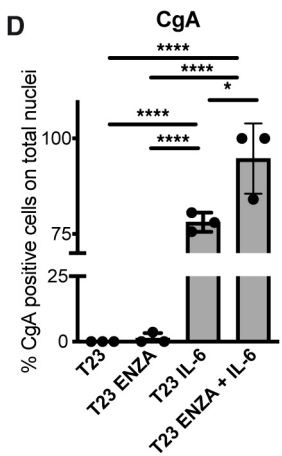

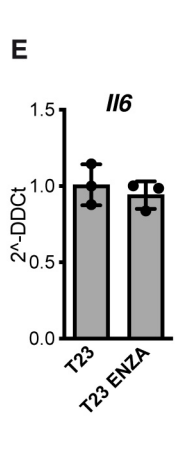

ENRIQUEZ, Supplementary FIGURE 9

Supplementary Figure 9. Exogenous IL-6 causes NED of adenocarcinoma cells. A and B. T23 prostate adenocarcinoma cell lines were cultured in the presence of 50 ng/ml of recombinant IL-6, of enzalutamide (ENZA), or their combination. Cells were collected after 5 days and analyzed by immunofluorescence for SYP (A) or CgA (B). **C and D.** Digital quantification of staining in A and B, respectively. **E.** Real time PCR for *Il6* in T23 cells treated or not with enzalutamide (ENZA). All histograms depict mean ± s.d. of biological replicates, indicated by dots. One-Way Anova: * $P < 0.05$, ** $P < 0.01$,*** $P < 0.001$, **** $P < 0.0001$. The experiment was repeated two times with comparable results.

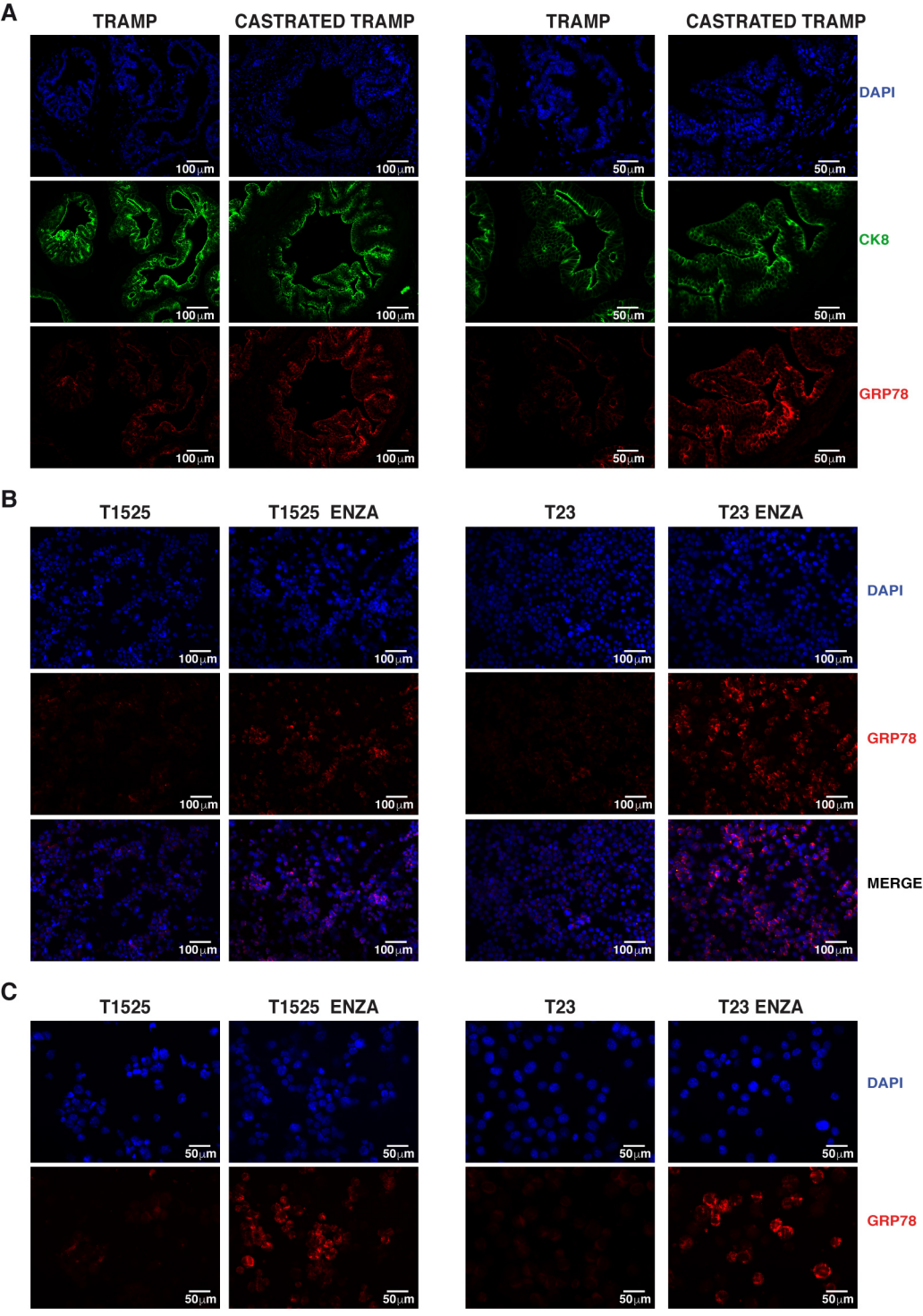

ENRIQUEZ, Supplementary FIGURE 10

Supplementary Figure 10. GRP78 is up-regulated in tumor cells upon castration or enzalutamide treatment. A. Separate channels of immunofluorescence reported in figure 6A. Green: CK8, red : GRP78, blue: DAPI. **B and C.** Enlarged fields (B) and separate channels (C) for immunofluorescence reported in figure 6D. Red: GRP78, Blue: DAPI.

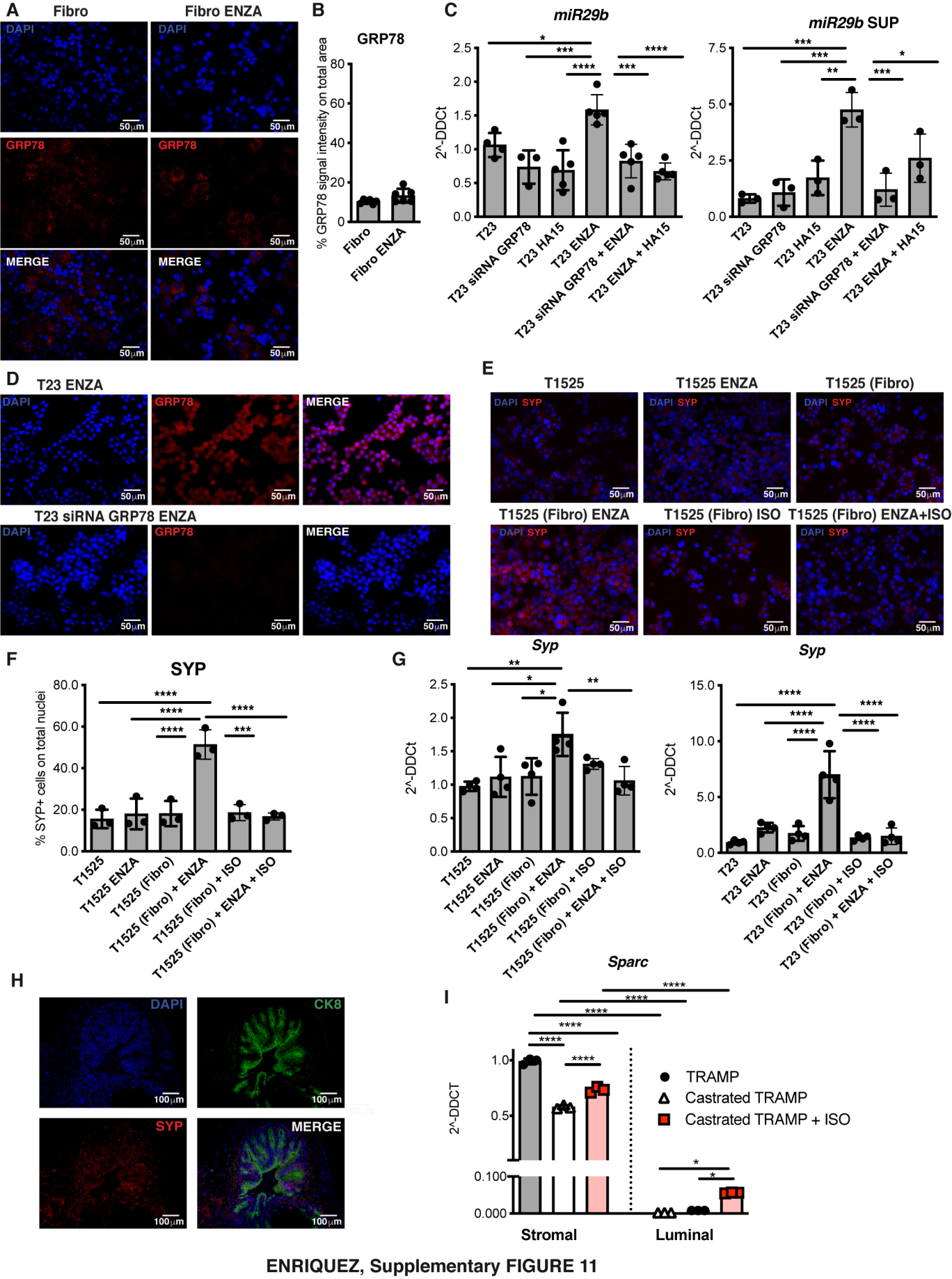

ENRIQUEZ, Supplementary FIGURE 11

Supplementary Figure 11. Isoliquiritigenin reduces NED and prevents SPARC down-regulation. A. Representative immunofluorescence for GRP78 (red) in murine wild type fibroblasts (Fibro) treated for 24h with enzalutamide (ENZA). Blue: DAPI. **B.** Quantification of staining in panel A. **C.** T23 cells were either transiently transfected with siRNA specific for GRP78, or cultured with HA15, a chemical specific inhibitor of GRP78. Where indicated cells were also treated with enzalutamide (ENZA) for 24h. Histograms show real time PCR for *miR-29b1* in cells (left panels) or in supernatants (right panel). Data are a pool of two independent experiments. **D.** Representative immunofluorescence for GRP78 (red) in T23 cells transfected with siRNA specific for GRP78 or in control cells, after treatment with enzalutamide (ENZA). Blue: DAPI **E-G.** T1525 or T23 prostate adenocarcinoma cell lines were co-cultured in transwell system with fibroblasts (Fibro, indicated in brackets) also adding enzalutamide (ENZA), isoliquiritigenin (ISO) or their combination where indicated, as depicted in Fig.6J. **E.** Representative immunofluorescence for SYP (red) in T1525 cells. Blue : DAPI. **F.** Quantification of E. **G.** Graphs report real time PCR for *Syp* on both T1525 and T23 tumor cells. Data are a pool of two independent experiments. **H.** Immunofluorescence staining for CK8 (green), SYP (red) and DAPI (blue) showing NED on a prostate of a TRAMP mouse treated with isoliquiritigenin (ISO). **I.** Real time PCR for *Sparc* on stromal and luminal cells sorted from the prostates of untreated and castrated TRAMP mice, the latter treated or not with ISO (n= 3 biological replicates/group).

All histograms depict mean ± s.d. of biological replicates, indicated by dots. One-Way Anova followed by Tukey's test: * $P < 0.05$, ** $P < 0.01$, **** $P < 0.0001$.

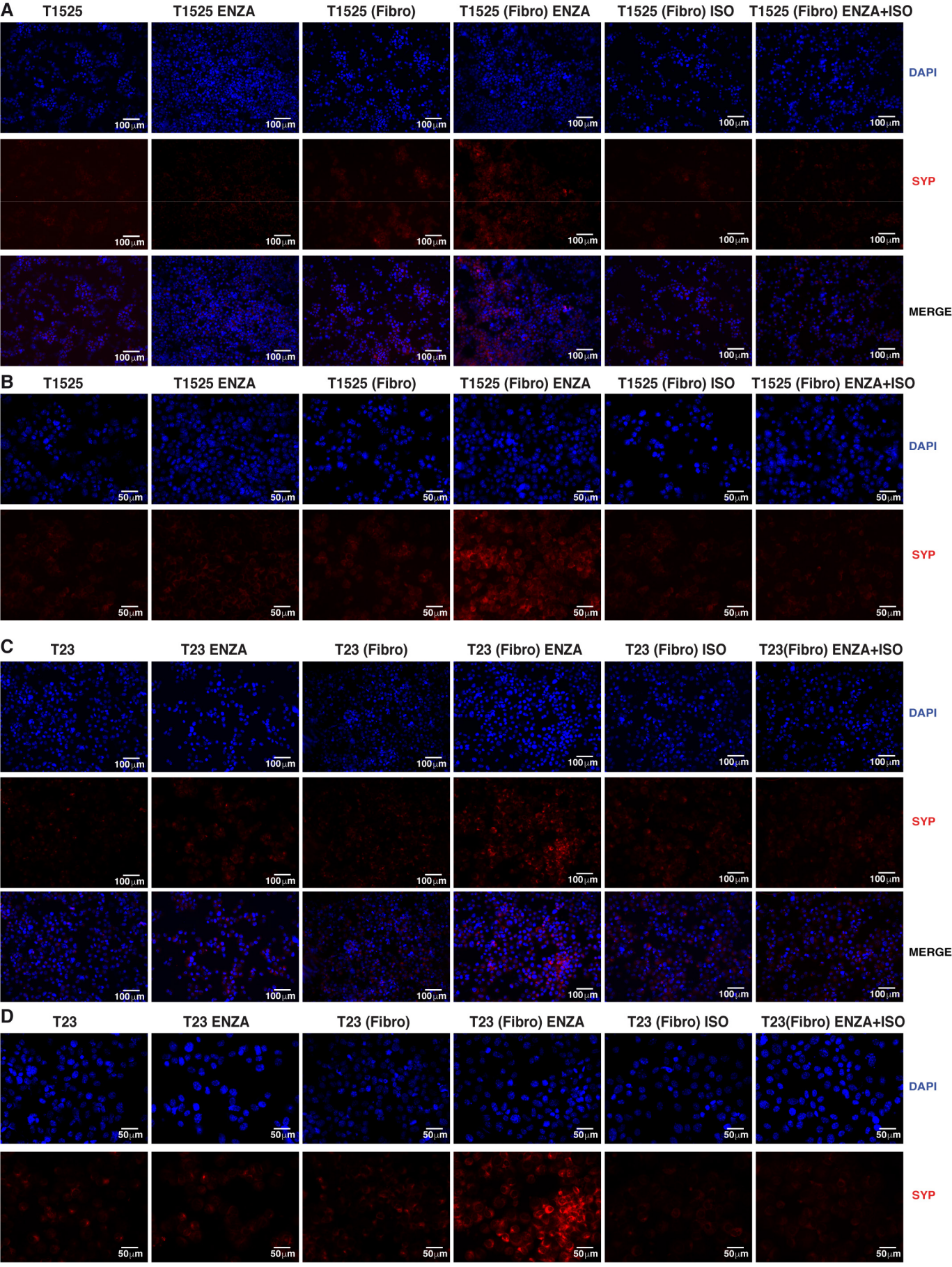

ENRIQUEZ, Supplementary FIGURE 12

Supplementary Figure 12. Only co-culture with fibroblasts induces NED of tumor cells when treated with enzalutamide. Enlarged fields (A and C) and separate channels (B and D) for immunofluorescence reported in figure 5J and S11E. Red: SYP, Blue: DAPI.

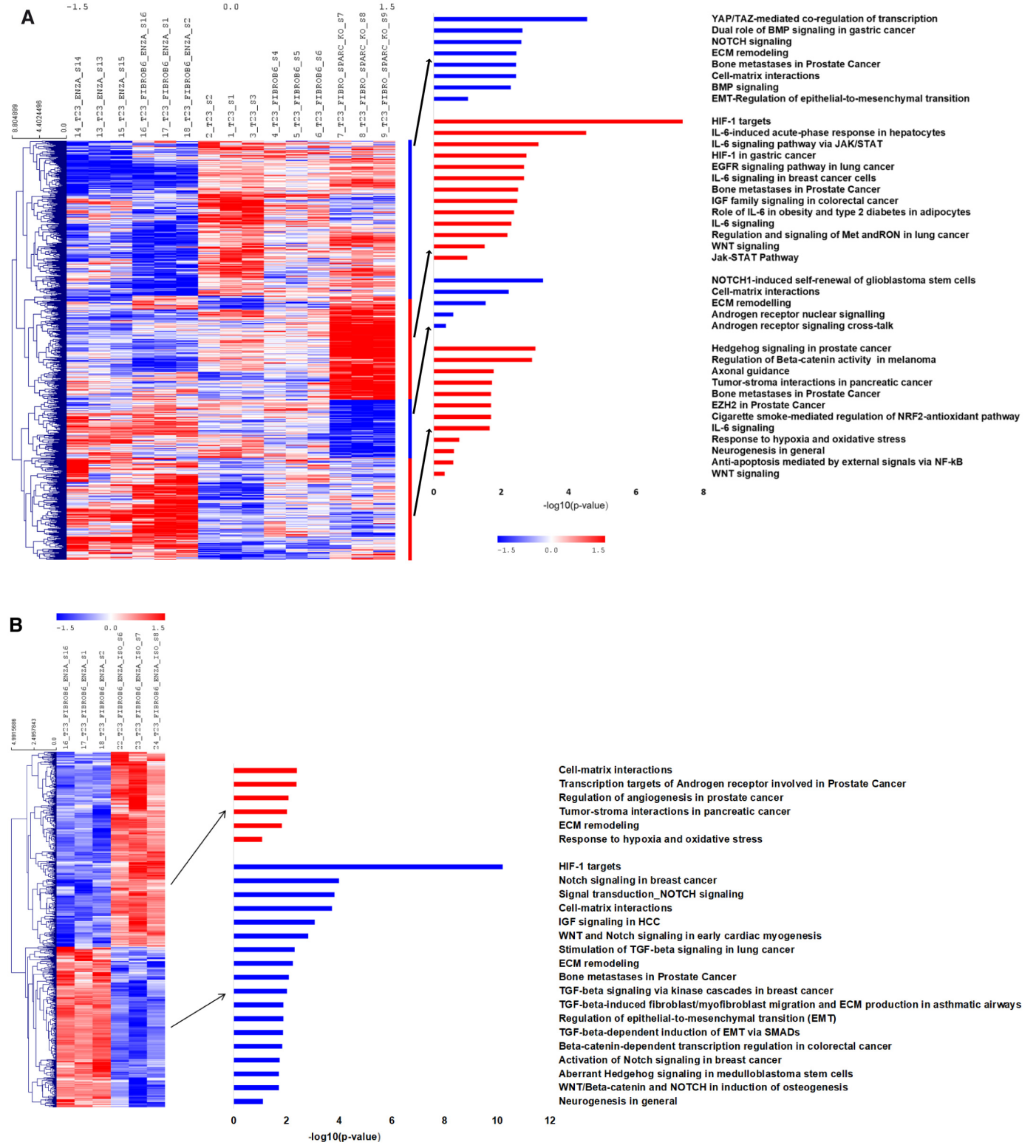

ENRIQUEZ, Supplementary FIGURE 13

Supplementary Figure 13. RNAseq analysis in T23 cells cultured with SPARC-proficient or deficient fibroblasts, and treated with enzalutamide, isoliquiritigenin or their combination.

A. Heatmap of the genes significantly up or down regulated (log2FC > 0.58 and Adj Pvalue < 0.05) in RNAseq experiments performed on T23 tumor cells, cultured alone or with wild type (Fibro) or SPARC-deficient (Fibro SparcKO) fibroblasts. Where indicated enzalutamide (ENZA) was added to the culture. On the right, bar plots show pathways significantly enriched by up-regulated (red bars) or down-reguated (blue bars) genes. **B** Heatmap of the genes significantly up or down regulated (log2FC > 0.58 and Adj Pvalue < 0.05) in RNAseq experiments performed on T23 tumor cells cultured with wild type fibroblasts (Fibro), in presence of enzalutamide (ENZA) or of enzalutamide (ENZA) and isoliquiritigenin (ISO). On the right, bar plots show pathways significantly enriched by up-regulated (red bars) or down-regulated (blue bars) genes.

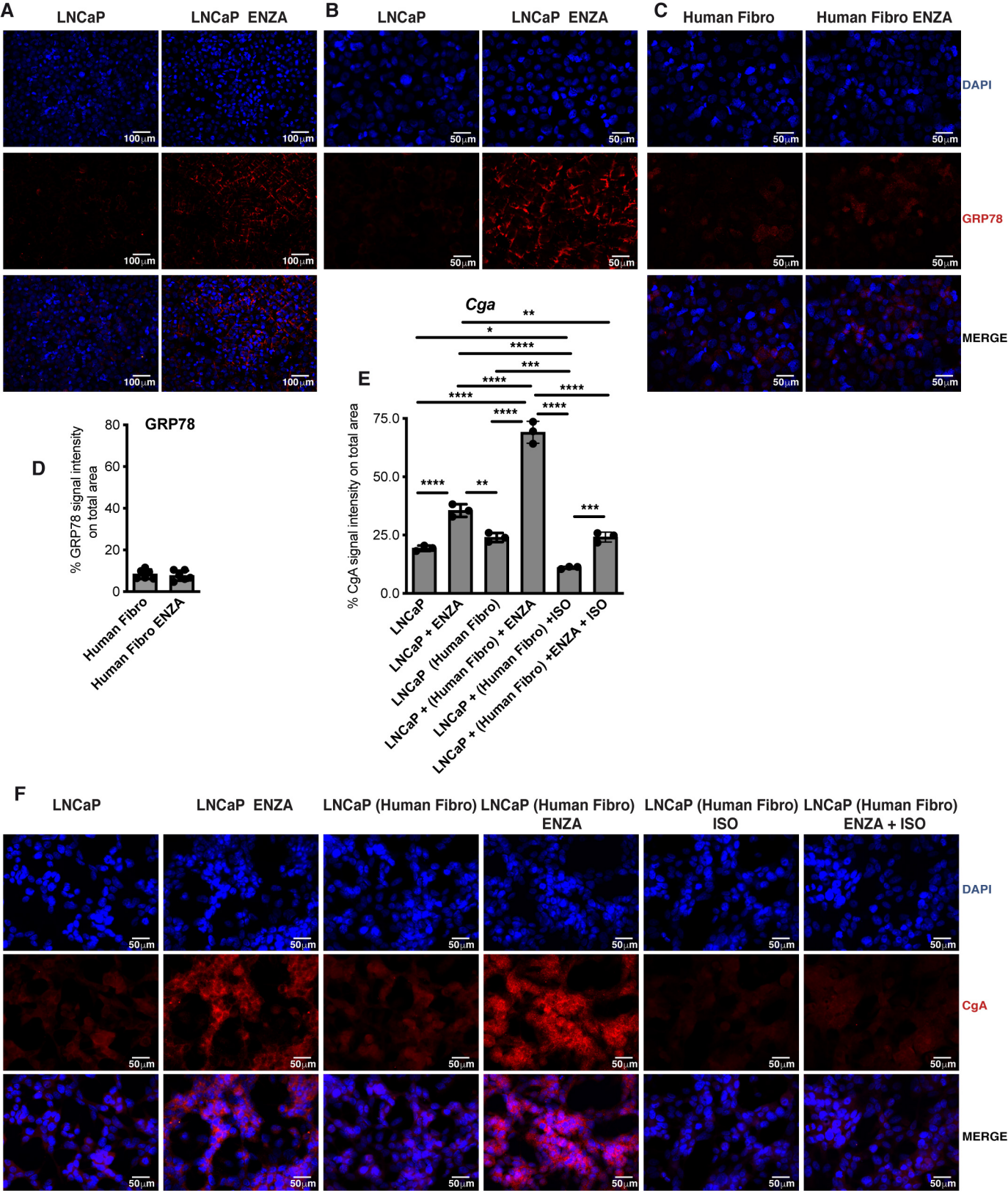

ENRIQUEZ, Supplementary FIGURE 14

Supplementary Figure 14. Down-regulation of SPARC in human fibroblast and up-regulation of CgA in LNCaP tumor cells after co-culture. A and B. Enlarged fields (A) and separate channels (B) for immunofluorescence reported in figure 7A. Red: GRP78, Blue: DAPI. Staining quantification for LNCaP is in figure 7B. **C.** Immunofluorescence for GRP78 (red) in human prostatic fibroblasts (the WPMY-1 cell line, indicated as Human Fibro) treated for 24h with enzalutamide (ENZA). **D.** Quantification of staining in panel C. Dots represent biological replicates **E.** Quantification of CgA staining reported in panel F. Histograms depict mean ± s.d. of biological replicates, indicated by dots. One-Way Anova followed by Tukey's test: * $P < 0.05$, ** $P < 0.01$, *** $P < 0.001$, **** $P < 0.0001$. **F.** Immunofluorescence for CgA (red; Blue signal is DAPI) in LNCaP cells co-cultured or not with human fibroblasts (indicated in brackets) and treated with enzalutamide (ENZA)., isoliquiritigenin (ISO) or their combination, as in figure 7I.

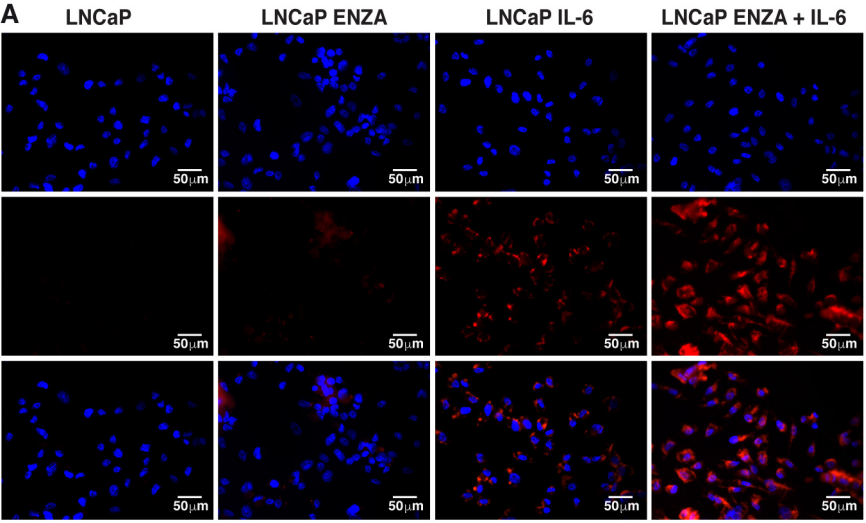

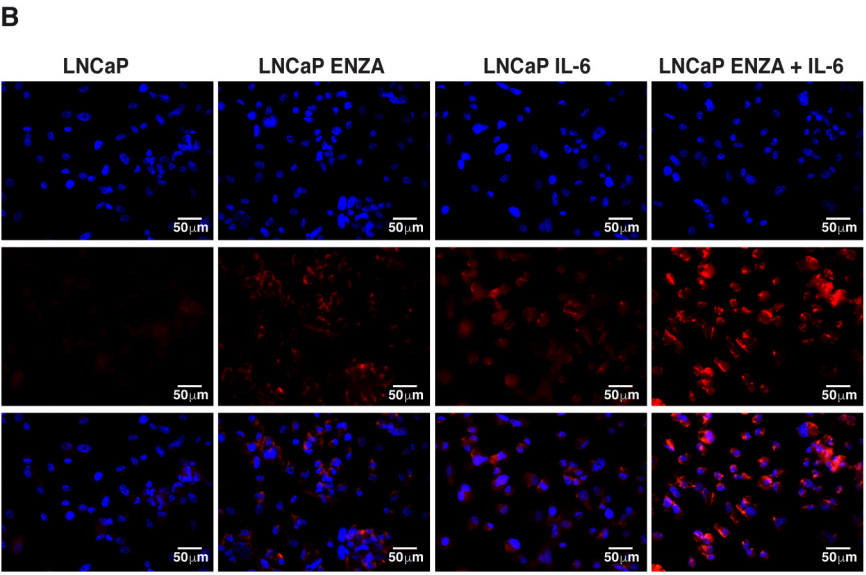

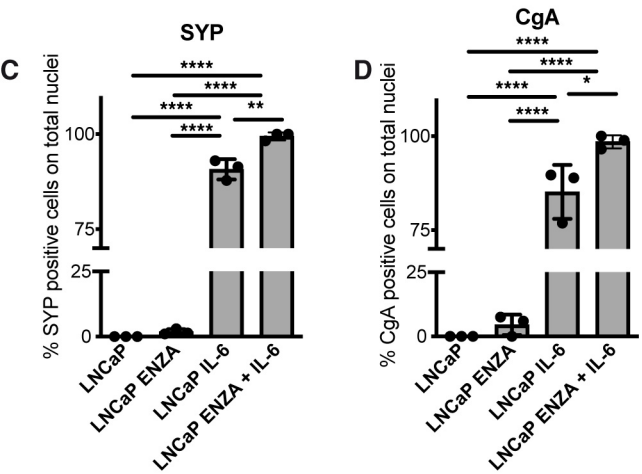

ENRIQUEZ, Supplementary FIGURE 15

Supplementary Figure 15. Exogenous IL-6 causes NED of LNCaP cells. A and B. LNCaP prostate adenocarcinoma cells were cultured in the presence of 50 ng/ml of recombinant IL-6, of enzalutamide (ENZA), or their combination. Cells were collected after 3 days and analyzed by immunofluorescence for SYP (A) or CgA (B). **C and D.** Digital quantification of staining in A and B, respectively. Histograms depict mean ± s.d. of biological replicates, indicated by dots. One-Way Anova followed by Tukey's test: * $P < 0.05$, ** $P < 0.01$,*** $P < 0.001$, **** $P < 0.0001$. The experiment was repeated two times with comparable results.

A

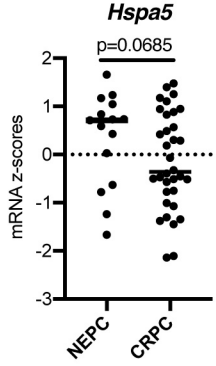

B

ID	Description	p value	REFERENCE
R-HSA-9614399	Regulation of localization of FOXO transcription factors	<1E-05	Qi, Cancer Cell, 2010, doi: 10.1016/j.ccr.2010.05.024
R-HSA-198323	AKT phosphorylates targets in the cytosol	<1E-05	Lee, Cancer Cell, 2016, DOI:https://doi.org/10.1016/j.ccell.2016.03.001; Dardenne, Cancer Cell, 2016, DOI http://dx.doi.org/10.1016/j.ccell.2016.09.005
R-HSA-1257604	PIP3 activates AKT signaling	<1E-05	Lee, Cancer Cell, 2016, DOI:https://doi.org/10.1016/j.ccell.2016.03.001; Dardenne, Cancer Cell, 2016, DOI http://dx.doi.org/10.1016/j.ccell.2016.09.005
R-HSA-9604323	Negative regulation of NOTCH4 signaling	<1E-05	Danza, Mol Cancer Res, 2012, DOI: 10.1158/1541-7786.MCR-11-0296
R-HSA-8854050	FBXL7 down-regulates AURKA during mitotic entry and in early mitosis	<1E-05	Beltran, Nature Medicine, 2016, doi: 10.1038/nm.4045
R-HSA-75815	Ubiquitin-dependent degradation of Cyclin D	<1E-05	Tsai, Cancer Res, 2015, DOI: 10.1158/1078-0432.CCR-15-0744
R-HSA-69610	p53-Independent DNA Damage Response	<1E-05	Zhang, Clin Cancer Res 2018, DOI: 10.1158/1078-0432.CCR-17-1872
R-HSA-69613	p53-Independent G1/S DNA damage checkpoint	<1E-05	Zhang, Clin Cancer Res 2018, DOI: 10.1158/1078-0432.CCR-17-1872
R-HSA-69615	G1/S DNA Damage Checkpoints	<1E-05	Zhang, Clin Cancer Res 2018, DOI: 10.1158/1078-0432.CCR-17-1872
R-HSA-2219528	PI3K/AKT Signaling in Cancer	4.26822E-09	Lee, Cancer Cell, 2016, DOI:https://doi.org/10.1016/j.ccell.2016.03.001
R-HSA-195721	Signaling by WNT	3.61772E-08	Davies, NatRevUrol, 2018, doi:10.1038/nrurol.2018.22

C

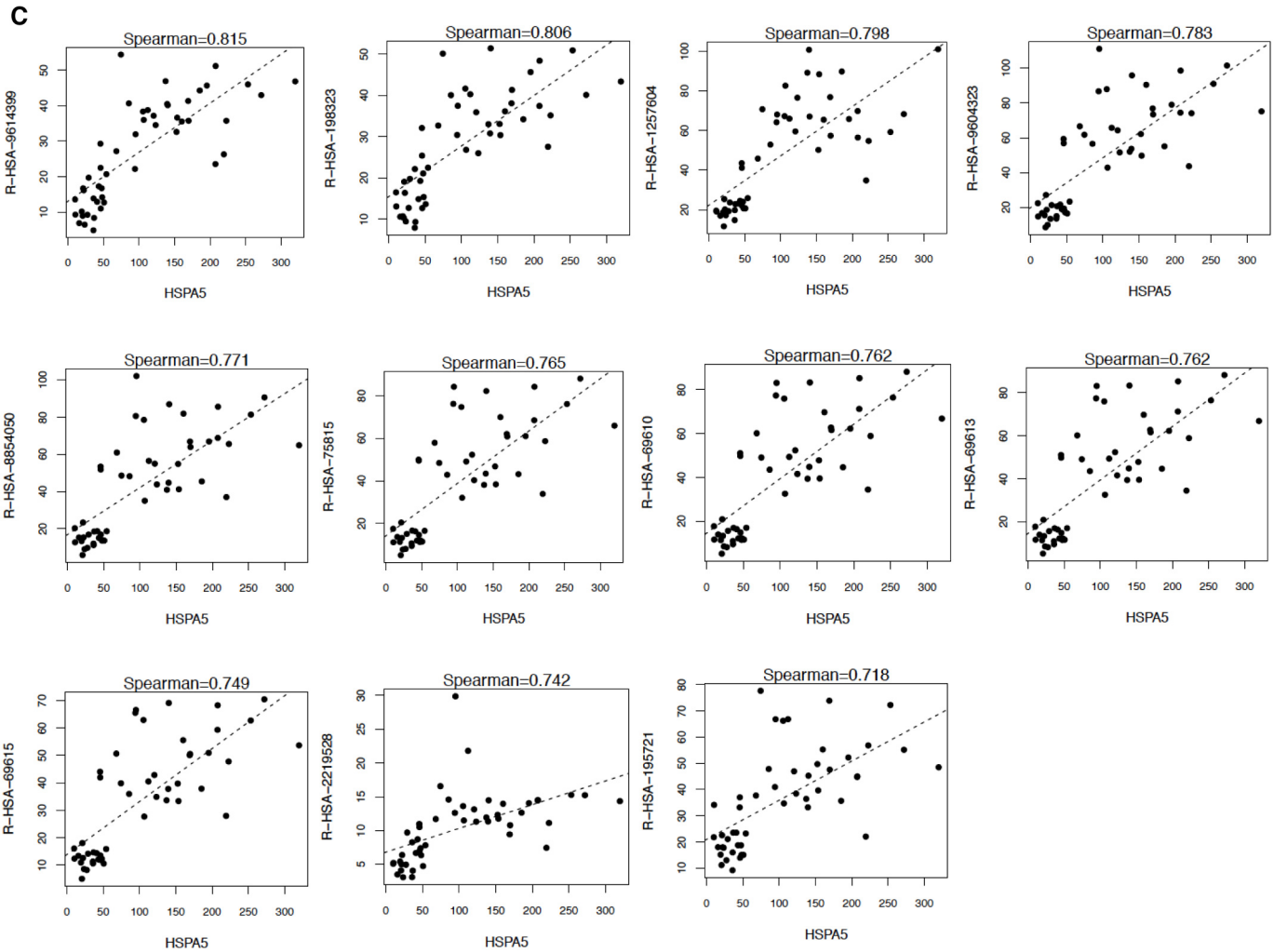

ENRIQUEZ, Supplementary FIGURE 16

Supplementary Figure 16. GRP78 correlation with pathways relevant in NE prostate cancer. A. Histogram shows the mRNA levels of Hspa5 in NEPC and CRPC patients in the Beltran data set. Z-scores were downloaded from the cBioPortal. One-tailed Student's t test was performed. **B.** List of pathways significantly positively correlated with *Hspa5* transcript expression in the Beltran data set**. C.** Scatterplots with spearman correlation between *Hspa5* (x-axis) and gene expression mean of indicated pathways (y-axis).

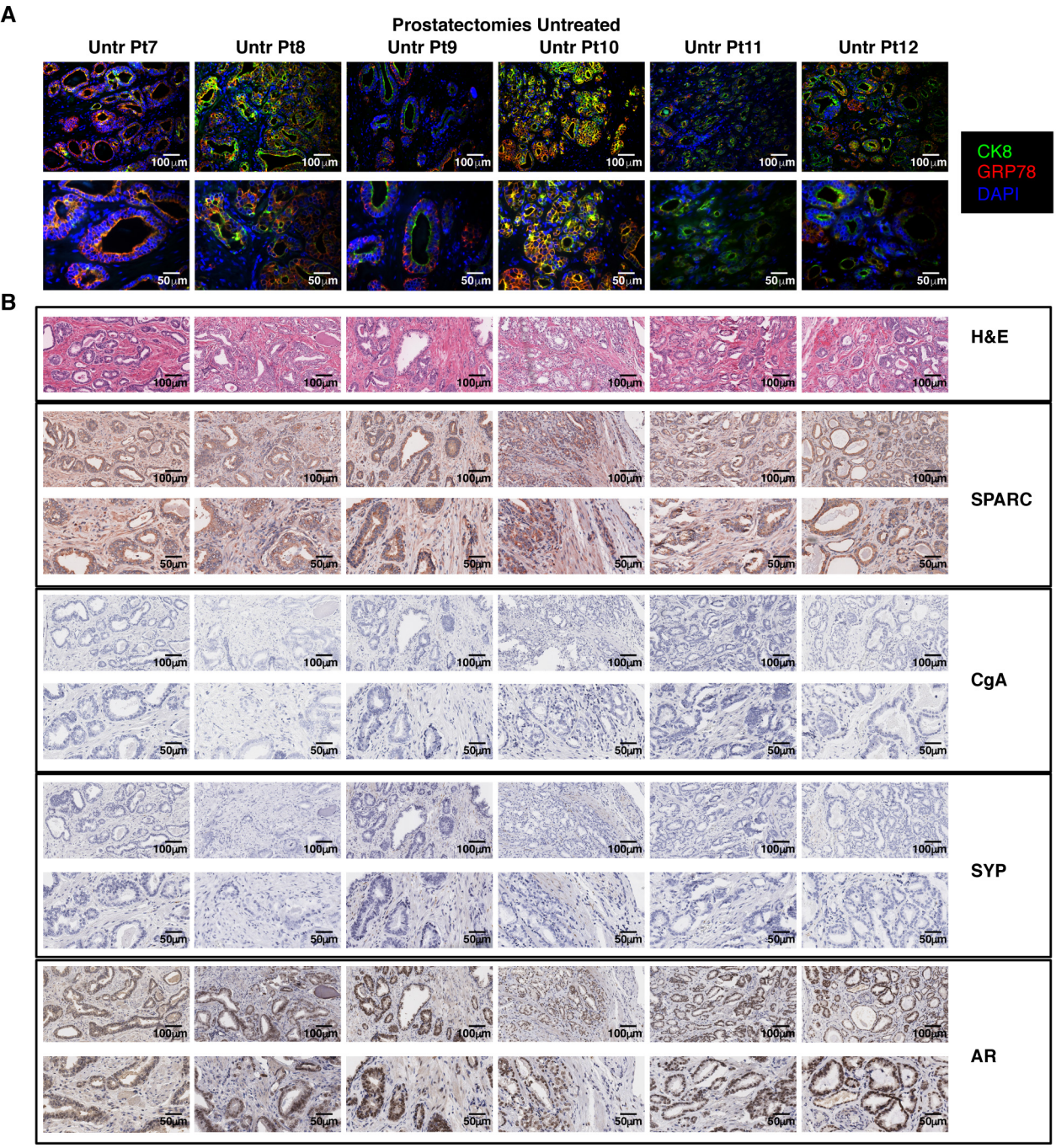

ENRIQUEZ, Supplementary FIGURE 17

Supplementary Figure 17. Immunofluorescence and immunohistochemistry in prostatectomies from untreated patients. A. Immunofluorescence staining for GRP78 (red) and DAPI (blue), and **B.** H&E staining and immunohistochemistry for SPARC, CgA, SYP and AR, in prostatectomies obtained from untreated prostate cancer patients.

A

ID patient	Neo-adjuvant Treatment	Duration of treatment (months)	Gleason Score
Pt1	Bicalutamide	4	3+4
Pt2	Enantone	5	3+4
Pt3	Casodex	7	4+3
Pt4	Eligard	5	4+4
Pt5	Enantone	5	4+3
Pt6	Casodex	7	3+4
Pt13	Bicalutamide	3	5+5
Pt14	Bicalutamide	7	3+3
UntrPt7	None	/	3+3
UntrPt8	None	/	4+5
UntrPt9	None	/	3+4
UntrPt10	None	/	4+5
UntrPt11	None	/	3+4
UntrPt12	None	/	3+5

B

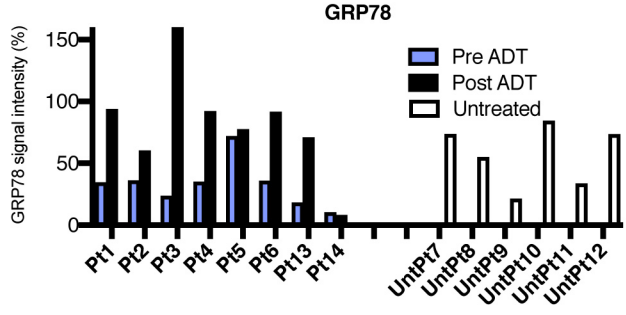

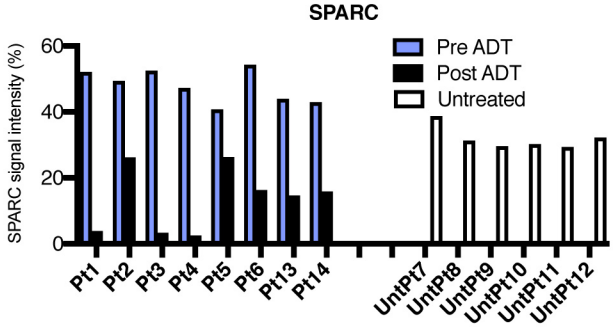

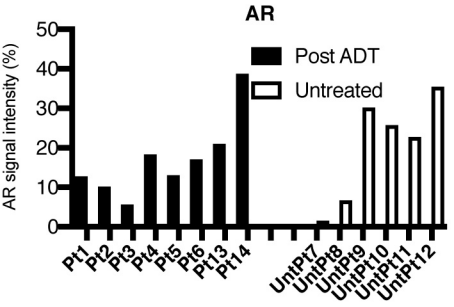

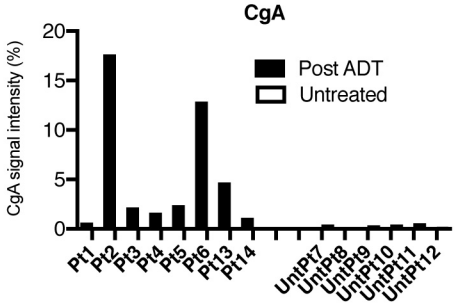

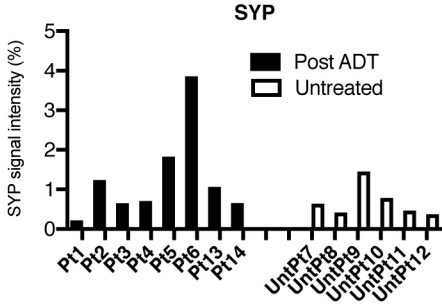

C

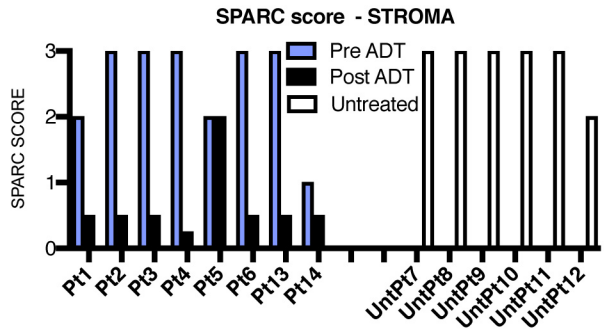

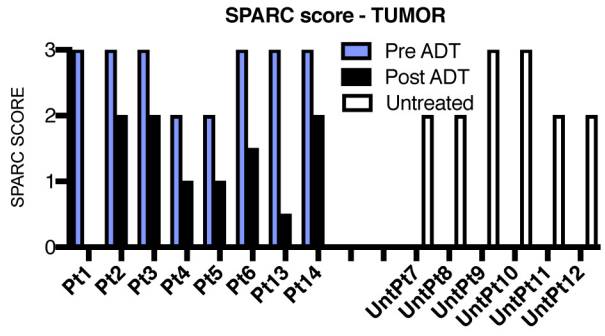

ENRIQUEZ, Supplementary FIGURE 18

Supplementary Figure 18. Characteristics of patients and quantifications of immunostaining on human tumor samples. A. Table reassuming the characteristics of the patients treated with neo-adjuvant ADT (Pt#1-6 and 13-14) and untreated control patients (UntrPt#7-12). **B.** Quantification of staining for GRP78, SPARC, AR, CgA and SYP reported in figure 8 and in supplementary figure 17. **C.** Score index assigned by pathologists to distinguish intensity of SPARC staining on stroma or tumor cells in the indicated patients. 0= no positivity, 3= maximum intensity.

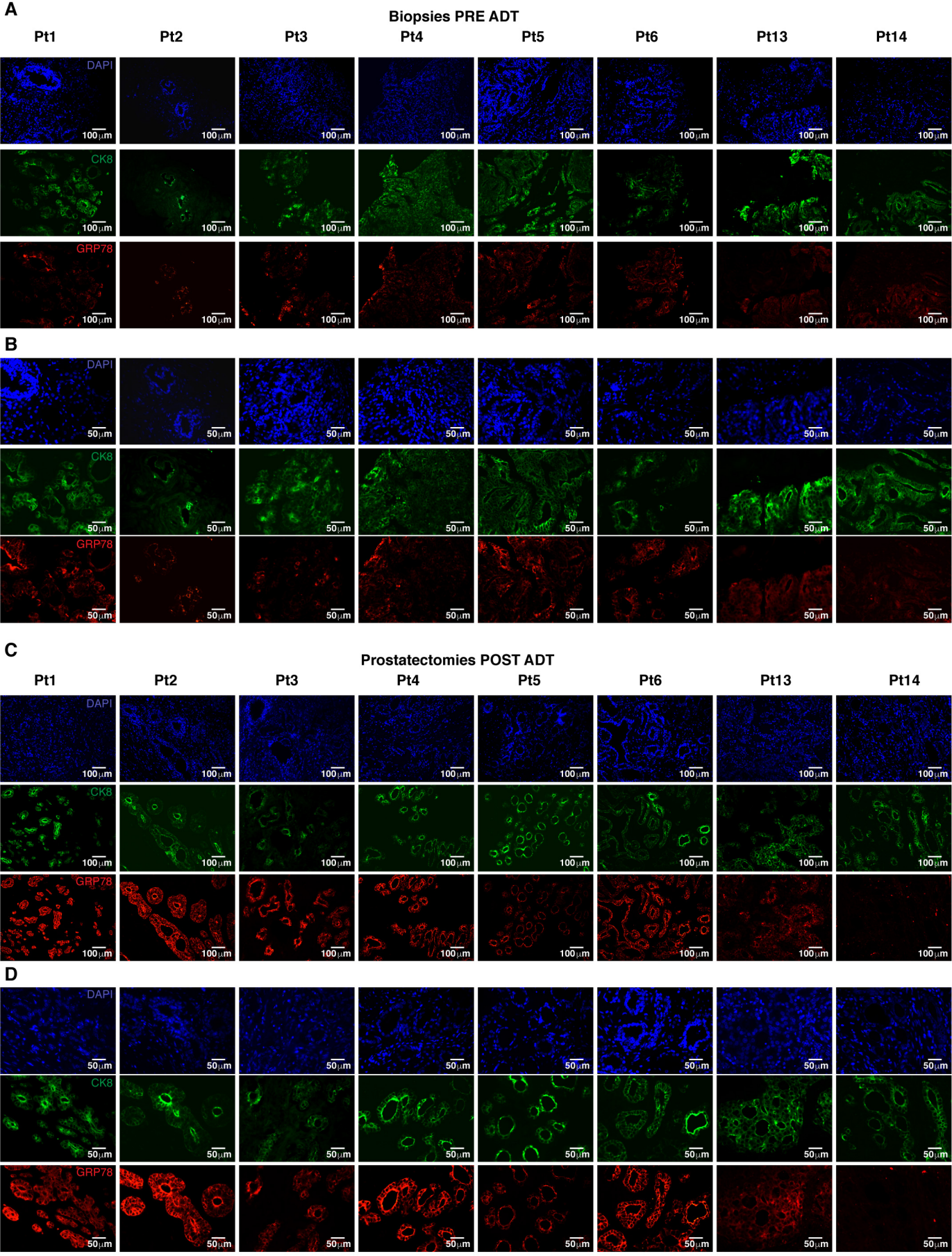

ENRIQUEZ, Supplementary FIGURE 19

Supplementary Figure 19. GRP78 immunofluorescence in prostate cancer tissue collected from patients pre and post ADT. A and B. Separate channels for immunofluorescence reported in figure 8A. Green: CK8, Red: GRP78, Blue: DAPI. **C and D.** Separate channels for immunofluorescence reported in figure 8B. Green: CK8, Red: GRP78, Blue: DAPI.

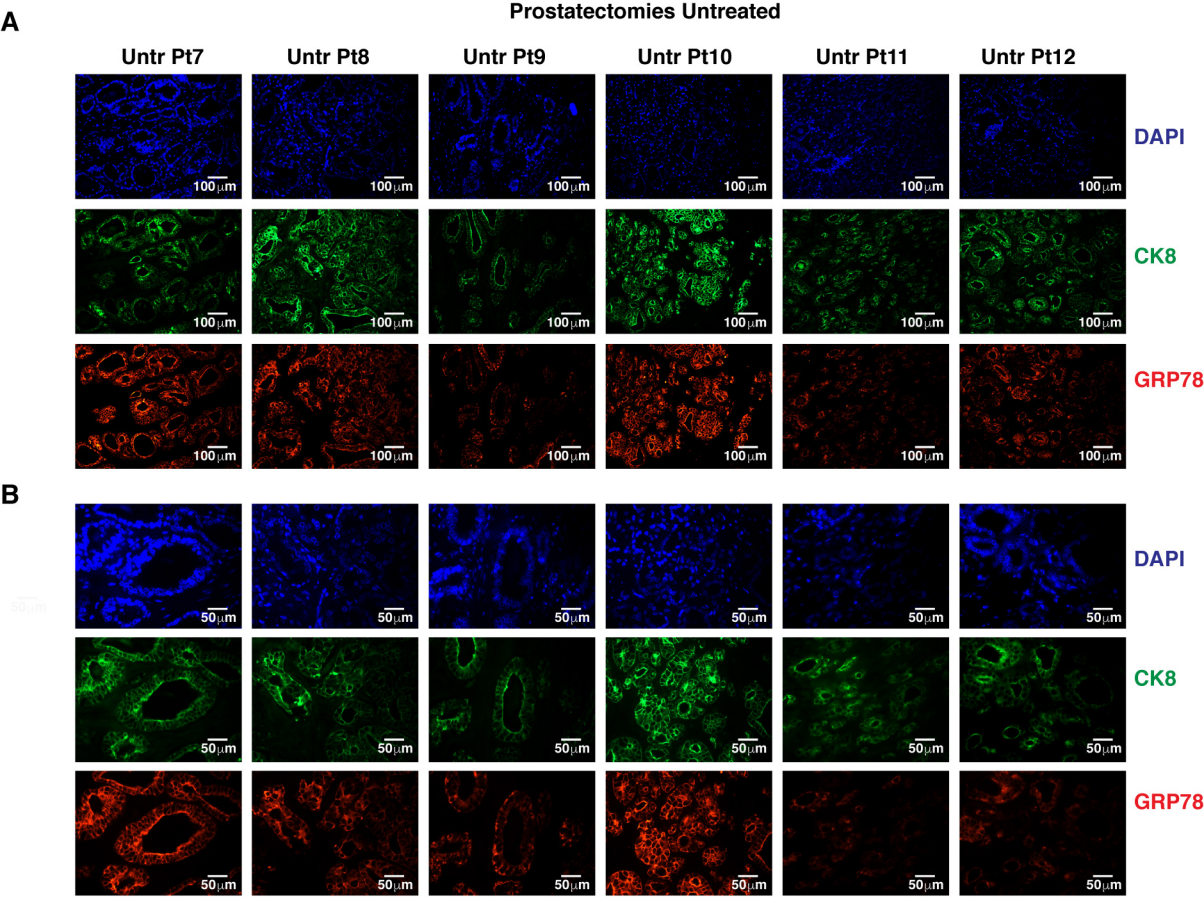

ENRIQUEZ, Supplementary FIGURE 20

Supplementary Figure 20. GRP78 immunofluorescence in prostate cancer tissue collected from untreated patients. Separate channels for immunofluorescence reported in supplementary figure 17A. Green: CK8, Red: GRP78, Blue: DAPI.